Research Square

Preprints are preliminary reports that have not undergone peer review.
They should not be considered conclusive, used to inform clinical practice,
or referenced by the media as validated information.

Radial Artery Pulse Wave Response to Submaximal Walking in Healthy Women with Obesity Phenotypes Manuscript Draft

Boncho Ku
Korea Institute of Oriental Medicine
Jang-Han Bae
Korea Institute of Oriental Medicine
Sangkwan Lee
Wonkwang University Gwangju Medical Center
Young-Ju Jeon
jyj92@kiom.re.kr

Korea Institute of Oriental Medicine

Article

Keywords: Radial pulse wave, android obesity, gynoid obesity, heart rate variability, submaximal exercise, premenopausal women

Posted Date: August 20th, 2026

DOI: https://doi.org/10.21203/rs.3.rs-9845354/v1

License: This work is licensed under a Creative Commons Attribution 4.0 International License. Read Full License

Additional Declarations: No competing interests reported.

Abstract

Background.

Body fat distribution may shape vascular function beyond overall adiposity. Whether radial pulse wave responses to acute exercise differ between android and gynoid obesity phenotypes in premenopausal women remains unclear.

Methods.

In this exploratory cross-sectional study, 42 premenopausal women aged 20–45 years were classified as normal-weight controls (; n = 13), with gynoid obesity (, ; n = 14), or with android obesity (, ; n = 15). Each participant completed a single-stage submaximal treadmill walking test; radial pulse waves, heart rate variability (HRV), and pulse analysis indices (pulse pressure index (PPI), pulse depth index (PDI), optimal applied pressure (OAP), and pulse tension index (PTI)) were measured immediately before and 3 minutes after exercise. Pre–post responses across phenotypes were compared with linear mixed-effects (LME) models.

Results.

Four outcomes showed significant stage × group interactions. Incisura height (H4) decreased in both obesity groups (Gynoid, ; Android,) but not in the controls (;). The PDI increased exclusively in the gynoid group (). PTIs at lower pressure thresholds (PTI20 and PTI30) decreased in the android group compared with the control group (and, respectively). Additional descriptive patterns not reaching interaction significance were consistent with phenotype-dependent responses but require confirmation.

Conclusions.

Both obesity groups exhibited exercise-induced H4 reductions that were absent in the controls, the android group showed divergent pulsatility responses (PTI20 and PTI30), and the gynoid group exhibited an uniquely increased PDI. These interaction-confirmed findings suggest that body fat distribution may shape peripheral hemodynamic responses to acute exercise, pending verification in larger studies with direct adipose quantification.

Introduction

Cardiovascular disease remains a major cause of morbidity and mortality, and excess adiposity is among its major modifiable risk factors[1,2]. Obesity affects not only total body mass but also body fat distribution. The distinction between android and gynoid obesity traces back to Vague's classic description of a predominantly upper-body pattern versus a lower-body pattern of fat accumulation; currently android fat generally refers to abdominal or upper-body adiposity, whereas gynoid fat refers more to gluteofemoral or lower-body fat deposition[3–5]. Classic epidemiologic and metabolic studies have shown that compared with generalized adiposity alone, central or upper-body fat accumulation is more strongly associated with adverse cardiometabolic outcomes[3,6–8]. Although body mass index (BMI) is widely used in clinical practice, it does not adequately distinguish between different obesity phenotypes. More direct characterization of regional adiposity is possible with imaging-based approaches, including dual-energy X-ray absorptiometry-derived android fat measurements and magnetic resonance imaging-derived estimates of visceral and abdominal subcutaneous fat depots[9,10]. However, such methods are not routinely deployed in clinical practice broadly, and BMI together with measures reflecting central fat distribution, such as waist circumference and the waist-to-hip ratio (WHR), remain widely used because these simple anthropometric indices still provide clinically useful information for cardiovascular risk assessment[5,10–13].

The vascular relevance of the obesity phenotype is supported by convergent evidence from endothelial, arterial stiffness, and subclinical atherosclerosis studies. In a randomized trial of healthy adults, short-term fat gain impaired brachial flow-mediated dilation, with a decrease in visceral rather than subcutaneous fat gain, indicating that regional fat contributes to early endothelial dysfunction before overt cardiometabolic disease[14]. Observational studies have similarly shown that indices of abdominal or visceral adiposity, such as WHR and visceral fat area, are associated with greater arterial stiffness and provide vascular information beyond BMI[15,16]. Visceral adipose tissue has also been shown to predict coronary artery calcification progression in prospective analysis, linking central adiposity to structural vascular injury[17]. Mechanistic reviews further indicate that visceral, more than subcutaneous, adipose expansion, drives inflammatory infiltration, vasoconstrictor signaling, endothelial dysfunction, and vascular stiffening[18]. In premenopausal women with obesity, radial pulse-wave-derived

endothelial dysfunction has also been linked to visceral obesity[19], reinforcing the rationale for phenotype-specific vascular evaluation in female populations.

Pulse wave analysis offers a noninvasive approach for evaluating vascular function. The palpation of the radial artery pulse has long served as a core clinical examination in traditional East Asian medicine, where it is used to infer systemic physiological states[20,21]. However, reviews of manual pulse diagnosis report variable interrater reliability, raising concerns about its reproducibility as a diagnostic tool, although reliability improves with operational definitions and standardized procedures[22]. To address these concerns, contemporary sensor-based acquisition of the radial pulse wave has been developed to translate this practice into reproducible quantitative features. Such single-site radial measurements are particularly attractive because the reference method for aortic stiffness, carotid-femoral pulse wave velocity, requires multisite measurements and experienced operators, which limits its routine use[23]. The radial artery pulse wave is more easily obtained and has been used to characterize arterial hemodynamics, estimate vascular stiffness, and support digital and wearable cardiovascular monitoring[20,23–25].

Acute exercise serves as a useful physiological probe: It transiently alters blood pressure, vascular function, and autonomic recovery[26–28], whereas exercise-induced increases in shear and circumferential stress directly influence vascular adaptation[29]. Pulse-wave responses during recovery may therefore reveal dynamic vascular reserve not captured at rest. This is especially relevant to adiposity research, as the favorable postexercise reduction in arterial stiffness attenuates with increased body fat[30], and obesity has been linked to paradoxical postexercise increases in central arterial stiffness even in young, otherwise healthy individuals[31]. However, evidence remains limited on whether radial pulse wave responses to submaximal exercise differ according to obesity phenotype, particularly in premenopausal women.

The present study aimed to compare radial artery pulse wave characteristics before and after a single-stage submaximal walking test among premenopausal women classified by obesity phenotype. On the basis of the evidence reviewed above, we hypothesized that android obesity, characterized by central adiposity and its associated vascular and autonomic burden, would show attenuated or divergent hemodynamic responses to exercise compared with normal-weight controls, whereas gynoid obesity might exhibit a distinct response pattern reflecting its relatively favorable cardiovascular profile. Because multidomain radial pulse wave responses to acute exercise have not been characterized across obesity phenotypes, this study was designed as an exploratory analysis across multiple pulse wave domains rather than a test of a single prespecified endpoint.

Materials and Methods

Ethics

This exploratory clinical study used a cross-sectional group-comparison design with repeated measurements obtained immediately before and after standardized single-session submaximal exercise stimulation. The exercise test was incorporated as a physiological provocation procedure to characterize acute hemodynamic responses rather than as a longitudinal therapeutic intervention. The study was conducted in accordance with the principles of the Declaration of Helsinki after approval by the institutional review board at the participating institution (approval number: WKIRB-2015/8), and written informed consent was obtained from all participants before any screening procedures were performed. Participant enrollment and data collection were carried out from September to December 2015.

Participants

Women aged 20 to 45 years living in Gwangju or Jeonnam, Republic of Korea, were screened for participation. Eligible participants were premenopausal women who completed the study procedures and were classified into one of three prespecified groups: a normal-weight control group ($18.5 \leq \ \mathrm{BMI} \ < 23.0\ \mathrm{kg/m^2}$), an android obesity group ($\mathrm{BMI} \ \geq \ 25.0\ \mathrm{kg/m^2}$ and $\mathrm{WHR} \ \geq \ 0.90$), and a gynoid obesity group ($\mathrm{BMI} \ \geq \ 25.0\ \mathrm{kg/m^2}$ and $\mathrm{WHR} \ < 0.85$). The BMI cutoff of $\geq \ 25.0\ \mathrm{kg/m^2}$ for obesity follows the Asia-Pacific classification for Asian populations[32,33]. The android-gynoid distinction follows the classification originally described by Vague[3], with WHR thresholds chosen within the range used in prior studies[34,35]. To preserve clear phenotypic contrast between android and gynoid fat distributions, women with intermediate WHR values from 0.85 to 0.90 were excluded; these cases were counted among the anthropometric ineligibility exclusions reported in the participant flow (Fig. 2).

The screening at Visit 1 included demographic assessment, vital signs, medical and medication history, menstrual history, alcohol and caffeine intake, anthropometry, and laboratory testing. Participants were excluded if they had evidence of uncontrolled cardiometabolic risk at screening, defined as a seated blood pressure $\geq \ 160/90$ mmHg after at least 3 minutes of rest, an low density lipoprotein (LDL)-cholesterol $\geq \ 160$ mg/dL, a triglyceride concentration $\geq \ 500$ mg/dL, or a fasting glucose concentration $\geq \ 126$ mg/dL. Additional exclusion criteria included endocrine disorders affecting body weight; major cardiovascular, pulmonary, malignant, renal, or hepatic disease; musculoskeletal or

rheumatic conditions that could limit treadmill exercise; pregnancy, lactation, or oral contraceptive use; irregular menstrual cycles during the previous 3 months; current smoking; body weight change of ≥ 5 kg within the previous month; recent participation in a weight-loss program or use of weight-loss medication; inability to perform the submaximal exercise test safely; and any other investigator-determined reason that made participation inappropriate. To minimize hormonal variability, Visit 2 was scheduled within 10 days after the onset of menstruation, targeting the follicular phase of the menstrual cycle.

Anthropometric Measurements

At Visit 2, baseline vital signs and anthropometric measurements were obtained before exercise. Height and weight were measured, and BMI was calculated. Waist circumference was measured at the natural indentation of the trunk, defined as the horizontal girth passing through the midpoint between the lowest rib and the iliac crest, read at the end of normal expiration. Hip circumference was measured at the level of the greatest posterior protrusion of the buttocks[36]. Both measurements were recorded to the nearest 0.1 cm; WHR was then derived for group classification. Additional circumference measurements included those of the neck, chest, upper arm, and thigh.

Biochemical and Hematology Tests

Biochemical and hematological tests were performed at the screening visit to confirm eligibility and to exclude participants with clinically important underlying disease; these tests were not treated as study outcomes. The screening panel covered hematology, renal and liver function, inflammatory markers, electrolytes, thyroid function, lipid profile, fasting glucose, and urinalysis. Urine pregnancy testing was additionally performed when applicable.

Single-Stage Submaximal Treadmill Walking Test

Participants were instructed to avoid alcohol, caffeine, and prolonged exercise before the test visit and to fast for at least 4 hours before Visit 2. On the test day, questionnaires, vital signs, and anthropometric measurements were completed first, followed by at least 30 minutes of seated rest. Pre-exercise radial artery pulse signals synchronized with electrocardiogram (ECG) signals were subsequently obtained.

The exercise challenge was a single-stage submaximal treadmill walking test based on the protocol of Ebbeling et al.[37]. Age-predicted maximal heart rate (HR) was estimated using the equation proposed by Nes et al.[38]:

$$\mathrm{HR}_{\max} = 211 - 0.64 \times \text{ age}.$$

The test consisted of a 2-minute warm-up at 3 kph and 0% grade, followed by a 4-minute stage at 0% grade with the speed individually adjusted between 3 and 7 kph to achieve 50–60% of the predicted speed $\mathrm{HR}_{\max}$. During the subsequent stage, the treadmill speed was fixed, and the grade was increased by 1% per minute to a maximum of 16% until 70% of the predicted $\mathrm{HR}_{\max}$ was reached. HR during exercise was monitored using a patient monitoring system, and the rating of perceived exertion was recorded during the final 5 seconds of each minute using the Borg CR10 scale. In accordance with the study protocol, the exercise laboratory was maintained at 21-23 $^{\circ}$ C and a relative humidity below 60%. After exercise, the same signal-acquisition procedure was repeated 3 minutes after test termination, and additional safety monitoring was performed thereafter.

Pulse Tonometric Device

Radial artery pulse signals were measured using a pulse tonometric device, KIOM-PAS ver. 2.0 (Korea Institute of Oriental Medicine, Republic of Korea). The device has been widely utilized in clinical studies, and several derived variables have demonstrated clinical relevance. Its reliability and safety were validated in accordance with clinical good manufacturing practice guidelines, whereas its electromechanical stability was certified on the basis of the IEC 60601-1 2nd edition standard. Pulse signals were acquired using a six-channel piezoresistive sensor array, and the channel exhibiting the highest signal amplitude was selected for subsequent analysis. The system employed a tonometric mechanism with a sampling rate of 1000 Hz, and both continuously acquired signals during applied pressure loading and a 60-second pulse recording obtained under constant applied pressure were used for analysis. Signal processing included smoothing using the weighted Henderson's moving average algorithm and noise reduction within the 0.005–30 Hz range using a Butterworth filter. All signal processing and waveform analyses were performed using LabVIEW 2016 (National Instruments, USA). Further details regarding the technical specifications and signal processing procedures have been described in our previous studies[39–41]. Concurrent ECGs for heart rate variability (HRV) analysis were acquired using the ECG100C module of a Biopac data acquisition system (Biopac Systems Inc., USA) with a standard 3-lead configuration; the analog output was routed to the DAQ channel of the KIOM-PAS system to enable simultaneous digitization with the radial pulse waveform.

Outcome Variables

The prespecified outcome variables are defined in Table 1. Briefly, the analysis set comprised three domains: HRV metrics, time-domain pulse waveform features, and pulse analysis indices. The HRV metrics included the mean normal-to-normal interval (NN), the standard deviation of the NN intervals (SDNN), the root mean square of successive differences (RMSSD), normalized low-frequency power (nLF; 0.04–0.15 Hz), normalized high-frequency power (nHF; 0.15–0.4 Hz), and the LF/HF ratio. The waveforms included T1, H1, H1w, T3, H3, T4, H4, T5, and H5, and the radial augmentation index corrected for an HR of 75 beats per minute (rAIx@75). The pulse analysis indices included the pulse pressure index (PPI), pulse depth index (PDI), optimal applied pressure (OAP), and pulse tension index (PTI). PTI was further classified into PTIp, where p denotes 20%, 30%, 50%, 70%, 80%, and 90% of the prespecified PPI threshold. The PTI quantifies the resistive force of pulse segments against the applied pressure; detailed descriptions are provided in the reference[41].

Table 1: Radial artery pulse wave outcome variables and units

Domain	Variable	Description	Unit
HRV metrics	NN	Mean NN interval	s
	SDNN	Standard deviation of NN intervals	ms
	RMSSD	Root mean square of successive differences	ms
	nLF	Low-frequency spectral power (0.04–0.15 Hz) normalized by total frequency	%
	nHF	High-frequency spectral power (0.15–0.4 Hz) normalized by total frequency	%
	LF/HF	(LF power)/(HF power)	
Pulse waveform features	T1	Rise time to the percussive wave	s
	H1	Percussive-wave amplitude	V
	H1w	Wave width at two-thirds of the percussive-wave height	s
	T3	Delay to the tidal wave	s
	H3	Tidal-wave height (radial augmentation index)	%
	T4	Ejection time to the incisura	s
	H4	Incisura height	%
	T5	Delay to the dicrotic wave	s
	H5	Dicrotic-wave height	%
	rAIx@75	Radial augmentation index standardized to 75 bpm	%
Pulse analysis indices	PPI	The voltage response of the sensor when the maximum pulse amplitude was reached	V
	PDI	Displacement of the sensor in the direction normal to the skin surface	mm
	OAP	Optimal applied pressure, where the pulse amplitude reached its maximum	V
	PTIp[a]	Sensor displacement between the maximum pulse amplitude point and the starting points with greater than p percentage of the maximum pulse amplitude	mm

[a]p = 20%, 30%, 50%, 70%, 80%, and 90% of PPI.

Statistical Analysis

Statistical analyses were performed using R (version 4.5.3)[42] with the derived study dataset. Continuous demographic and anthropometric variables are summarized as the mean $\pm$ standard deviation (SD), and categorical variables as number (percentage). Between-group comparisons for baseline characteristics were performed using one-way analysis of variance for continuous variables and Fisher's exact test for categorical variables. Hemodynamic outcome variables are summarized as the mean $\pm$ SD by obesity phenotype group and measurement stage.

Linear mixed-effects (LME) models were employed separately for each outcome variable with a participant-specific random intercept. Fixed effects included measurement stage (before vs. after exercise), obesity phenotype, baseline value, time interval between the preexercise and postexercise pulse wave measurements, and two-way interactions of stage with each of these covariates. Baseline values were included as

covariates to account for preexisting between-group heterogeneity in this nonrandomized design[43,44]. Stage-by-covariate interactions were retained to allow covariate effects to differ between conditions. Waveform-derived outcomes with marked right-skewness were log-transformed prior to modeling; for variables containing zero values, a log(1 + y) transformation was applied instead.

Estimated marginal means (EMMs) were derived from each LME model using the *emmeans* package[45]. For log(y) or log(1 + y) transformed outcomes, the EMMs and contrasts were back-transformed to the response scale. Within each obesity phenotype, the before-to-after exercise change was tested using pairwise contrasts of EMMs across stages. Between-group differences at each stage were evaluated using pairwise contrasts of the EMMs across obesity phenotypes. Because baseline values and measurement intervals were included as covariates, the postexercise between-group contrasts can be interpreted as baseline-adjusted between-group differences in the exercise response, conditional on the included covariates. Pairwise contrasts were adjusted for multiplicity by Tukey's method, with no additional adjustment across all outcomes given the exploratory nature of the analysis. Standardized effect sizes (Cohen's d) for within-group (before vs. after exercise) changes and for between-group differences in exercise-induced changes were derived from the t statistic and residual degrees of freedom of the corresponding LME pairwise contrasts, with two-sided 95% confidence intervals computed from the noncentral t distribution[46]. All tests were two-sided, and $p < 0.05$ was considered to indicate statistical significance.

Results

Participant Flow and Analysis Set

The participant flow from screening to the final analysis set is summarized in Fig. 2. A total of 82 women were screened for eligibility, of whom 25 were excluded for the following reasons: Anthropometric ineligibility (n = 7), cardiometabolic or laboratory abnormalities (n = 7), menstrual irregularity (n = 5), scheduling or availability constraints (n = 3), age ineligibility (n = 1), underlying disease (n = 1), and pregnancy (n = 1). The remaining 57 participants were classified into three groups according to their BMI and WHR: A normal-weight control group (n = 21), a gynoid obesity group (n = 17), and an android obesity group (n = 19).

After the submaximal treadmill walking test, participants were further excluded from the analysis for the following reasons. In the control group, eight participants were excluded: Three withdrew during the exercise test, one violated the inclusion/exclusion criteria identified after enrollment, one had a protocol violation, one produced abnormal measurement data, and two had excessive missing baseline outcome data ($\geq$ 50% of the 25 hemodynamic variables were missing at the preexercise timepoint). In the gynoid obesity group, three participants were excluded: One for a protocol violation, one for abnormal data, and one for excessive missing baseline data. In the android obesity group, four participants were excluded: One withdrew during exercise, one had a protocol violation, one produced abnormal data, and one had excessive missing baseline data.

The final analysis set therefore included 42 participants: 13 in the control group, 14 in the gynoid obesity group, and 15 in the android obesity group.

Participant Characteristics

The baseline characteristics of the 42 participants are summarized by obesity phenotype group in Table 2. The three groups did not differ in terms of age, height, resting blood pressure, pulse rate, or lifestyle factors (caffeine, alcohol, physical activity; all $p > 0.08$). As expected, body weight, BMI, waist circumference, hip circumference, and WHR differed significantly (all $p < 0.001$). The two obesity groups had comparable BMI values (gynoid, 27.0 ± 1.9; android, 27.8 ± 3.9 kg/m ^{2}) but differed in fat distribution: the android group had a greater waist circumference (96.0 ± 8.8 vs. 83.6 ± 6.6 cm) and a greater WHR (0.93 ± 0.03 vs. 0.80 ± 0.04).

Table 2
Participant characteristics by obesity phenotype Group

Characteristic	Control N = 13[1]	Gynoid N = 14[1]	Android N = 15[1]	p value[2]
Age [yr]	33.31 (7.99)	33.79 (8.62)	36.43 (6.98)	0.524
Systolic BP [mmHg]	112.69 (9.46)	113.64 (6.74)	114.67 (9.35)	0.833
Diastolic BP [mmHg]	74.46 (7.25)	73.21 (8.26)	79.47 (7.62)	0.082
Pulse [bpm]	73.54 (16.39)	79.21 (11.45)	72.07 (7.36)	0.261
Height [cm]	161.45 (4.13)	160.17 (5.13)	160.47 (4.17)	0.745
Weight [kg]	54.78 (4.69)	69.35 (6.50)	71.70 (11.50)	< 0.001
BMI [kg/m²]	21.01 (1.41)	27.01 (1.88)	27.79 (3.90)	< 0.001
Waist [cm]	72.60 (5.95)	83.64 (6.60)	96.00 (8.85)	< 0.001
Hip [cm]	95.03 (3.37)	104.01 (4.61)	103.03 (7.12)	< 0.001
Waist to hip ratio	0.76 (0.05)	0.80 (0.04)	0.93 (0.03)	< 0.001
Caffeine	9/13 (69%)	10/14 (71%)	13/15 (87%)	0.491
Alcohol	10/13 (77%)	6/14 (43%)	9/15 (60%)	0.197
GPAQ activity index				0.903
Low	3/13 (23%)	5/14 (36%)	6/15 (40%)	
Moderate	3/13 (23%)	2/14 (14%)	2/15 (13%)	
High	7/13 (54%)	7/14 (50%)	7/15 (47%)	
Time interval between pre- and postexercise pulse wave measurements (min)	37.54 (14.34)	36.43 (6.10)	36.87 (6.65)	0.955

[1]Mean (SD); n/N (%)

[2]One-way analysis of means; Fisher's exact test; Pearson's Chi-squared test

HRV Metrics

HRV responses to submaximal walking are summarized in Table 3 and Fig. 3. No significant stage × group interactions were observed for any HRV index, although nLF showed a borderline interaction ($p_{int} = 0.068$); all the other interactions were nonsignificant (all $p_{int} > 0.14$).

Submaximal walking produced uniform time-domain responses across groups: the NN interval and RMSSD decreased significantly in all three groups (all $p < 0.001$), with no between-group differences (all $p > 0.16$).

The frequency of domain responses differed by phenotype. The Control and Gynoid groups exhibited the expected sympathovagal shift (nLF increased, nHF decreased, LF/HF rose; all $p \leq 0.003$), whereas the Android group showed no significant change in any frequency domain index (all $p > 0.21$). Postexercise, the nLF of the Android group was significantly lower than that of both the Control (MD $= -13.3\backslash\%$, $p = 0.013$; $d = -0.69$) and Gynoidgynoid (MD $= -11.9\backslash\%$, $p = 0.020$; $d = -0.65$) groups, with correspondingly higher nHF (Android vs. Gynoid: $p = 0.032$; $d = 0.61$).

Table 3
Responses of HRV metrics to submaximal walking by obesity phenotype

		Control		Gynoid		Android		Gynoid - Control	Android - Control	Android - Gynoid	
Features	**Adj. BL**	**Unadj.BL Mean (SD)**	**Change (95% CI)**	**Unadj.BL Mean (SD)**	**Change (95% CI)**	**Unadj.BL Mean (SD)**	**Change (95% CI)**	**MD (95% CI)**	**MD (95% CI)**	**MD (95% CI)**	**p_{int}**
NN [s]†	0.85	0.88 (0.17)	-0.08 ▯ (-0.12, -0.05)	0.82 (0.12)	-0.09 ▯ (-0.13, -0.06)	0.88 (0.07)	-0.08 ▯ (-0.11, -0.04)	-0.01 (-0.05, 0.03)	0.01 (-0.03, 0.05)	0.01 (-0.03, 0.05)	0.826
SDNN [ms]†	34.2	40.6 (18.3)	-7.66 ▯ (-12.7, -2.61)	28.4 (11.6)	-3.25 (-8.53, 2.04)	45.0 (17.9)	-4.11 (-9.07, 0.86)	4.41 (-1.35, 10.2)	3.55 (-1.84, 8.94)	-0.86 (-6.96, 5.24)	0.371
RMSSD [ms]†	28.0	35.5 (14.1)	-11.0 ▯ (-15.4, -6.57)	23.0 (13.3)	-8.33 ▯ (-12.9, -3.78)	36.9 (18.2)	-8.97 ▯ (-13.1, -4.81)	2.66 (-1.70, 7.02)	2.02 (-1.89, 5.92)	-0.65 (-5.17, 3.88)	0.534
nLF [%]	43.7	39.1 (19.0)	15.9 ▯ (6.47, 25.3)	44.4 (13.2)	14.5 ▯ (5.88, 23.1)	47.3 (20.9)	2.55 (-5.97, 11.1)	-1.37 (-12.2, 9.48)	-13.3 ▯ (-24.2, -2.41)	-11.9 ▯ (-22.3, -1.57)	0.068
nHF [%]	49.7	50.3 (17.0)	-14.3 ▯ (-23.3, -5.35)	50.1 (12.9)	-15.6 ▯ (-23.9, -7.31)	48.6 (19.3)	-4.86 (-13.0, 3.32)	-1.29 (-11.7, 9.12)	9.47 • (-0.91, 19.9)	10.8 ▯ (0.77, 20.8)	0.143
LF/HF†	0.82	1.07 (1.03)	1.05 ▯ (0.38, 1.71)	1.01 (0.55)	0.90 ▯ (0.32, 1.47)	1.26 (0.83)	0.25 (-0.15, 0.65)	-0.15 (-1.12, 0.81)	-0.80 • (-1.63, 0.03)	-0.64 • (-1.38, 0.09)	0.153

Adj. BL: LME model-adjusted baseline value; Unadj. BL: Unadjusted baseline Mean (SD); MD: Mean difference of changes between groups; p_{int}: p value based on F test for the interaction between stage and obesity phenotype in the LME model; pairwise contrast p values were adjusted for multiplicity using Tukey's HSD.

† log-transformed; ‡ log1p-transformed in model; For log or log(1 + y)-transformed outcomes, all EMMs and contrasts were back-transformed to the response scale.

• p < .10; ▯ p < .05; ▯ p < .01; ▯ p < .001.

Pulse Waveform Features

Among the ten time-domain pulse waveform features (Table 4; Fig. 4), only H4 exhibited a significant stage × group interaction ($p_{int} = 0.002$); all the other interaction terms were nonsignificant (all $p_{int} > 0.31$).

H4 decreased in both obesity groups (Gynoid, -6.87%, $p < 0.001$, $d = -0.53$; Android, -4.33%, $p = 0.006$, $d = -0.34$) but not in controls ($+1.03\%$, $p = 0.525$), yielding large between-group effect sizes (Gynoid vs. Control: $d = -1.17$; Android vs. Control: $d = -0.79$). The rAIx@75 decreased significantly in the Gynoid group (-11.8%, $p = 0.018$), with a similar trend in the Android group (-8.18%, $p = 0.087$), but not in the Control group ($p = 0.547$); the stage × group interaction for rAIx@75 was not significant ($p_{int} = 0.470$). No significant changes or between-group differences were detected for the remaining waveform features (all $p_{int} > 0.31$).

Table 4
Responses of time-domain pulse waveform features to submaximal walking by obesity phenotype

		Control		Gynoid		Android		Gynoid - Control	Android - Control	Android - Gynoid	
Features	**Adj. BL**	**Unadj.BL Mean (SD)**	**Change (95% CI)**	**Unadj.BL Mean (SD)**	**Change (95% CI)**	**Unadj.BL Mean (SD)**	**Change (95% CI)**	**MD (95% CI)**	**MD (95% CI)**	**MD (95% CI)**	**p_{int}**
T1 [s]†	0.10	0.10 (0.03)	0.01 (-0.00, 0.02)	0.11 (0.03)	0.00 (-0.01, 0.01)	0.10 (0.02)	0.01 ▯ (0.00, 0.03)	-0.01 (-0.02, 0.01)	0.01 (-0.01, 0.02)	0.01 • (-0.00, 0.03)	0.319
H1 [V]†	2.67	2.89 (0.79)	0.19 (-0.24, 0.62)	2.70 (0.73)	0.17 (-0.23, 0.57)	2.68 (0.60)	-0.19 (-0.55, 0.18)	-0.02 (-0.54, 0.50)	-0.38 (-0.87, 0.12)	-0.35 (-0.82, 0.11)	0.316
H1w [s]	0.18	0.19 (0.03)	0.00 (-0.02, 0.02)	0.17 (0.04)	-0.01 (-0.03, 0.01)	0.19 (0.04)	-0.00 (-0.02, 0.02)	-0.01 (-0.04, 0.01)	-0.00 (-0.03, 0.02)	0.01 (-0.01, 0.03)	0.602
T3 [s]	0.22	0.21 (0.05)	0.02 (-0.00, 0.04)	0.23 (0.03)	0.01 (-0.01, 0.04)	0.22 (0.02)	-0.01 (-0.03, 0.02)	-0.00 (-0.03, 0.02)	-0.02 (-0.05, 0.00)	-0.02 (-0.04, 0.01)	0.418
H3 [%]	71.9	73.1 (17.2)	-0.16 (-9.31, 8.98)	67.0 (10.8)	-8.27 • (-17.4, 0.83)	75.3 (13.1)	-4.12 (-12.7, 4.42)	-8.11 (-19.3, 3.06)	-3.96 (-14.7, 6.83)	4.15 (-6.66, 15.0)	0.464
T4 [s]	0.31	0.31 (0.04)	0.02 ▯ (0.00, 0.03)	0.32 (0.03)	0.03 ▯ (0.01, 0.04)	0.31 (0.03)	0.01 • (-0.00, 0.03)	0.01 (-0.01, 0.03)	-0.00 (-0.02, 0.02)	-0.01 (-0.03, 0.01)	0.503
H4 [%]	40.8	39.7 (9.91)	1.03 (-2.19, 4.26)	39.5 (7.12)	-6.87 ▯ (-9.92, -3.82)	42.7 (9.47)	-4.33 ▯ (-7.34, -1.31)	-7.90 ▯ (-11.7, -4.10)	-5.36 ▯ (-9.19, -1.52)	2.54 (-1.15, 6.24)	0.002
T5 [s]	0.26	0.30 (0.14)	-0.02 (-0.11, 0.06)	0.27 (0.18)	0.05 (-0.03, 0.12)	0.21 (0.18)	0.00 (-0.08, 0.08)	0.07 (-0.03, 0.17)	0.03 (-0.08, 0.13)	-0.04 (-0.14, 0.05)	0.502
H5 [%]‡	1.30	3.77 (6.89)	-0.41 (-1.19, 0.37)	1.79 (1.84)	-0.24 (-0.99, 0.52)	2.14 (4.57)	-0.11 (-0.88, 0.66)	0.18 (-0.68, 1.03)	0.30 (-0.60, 1.20)	0.12 (-0.76, 1.01)	0.846
rAIx@75 [%]	73.0	73.4 (21.3)	-3.09 (-13.3, 7.10)	67.5 (11.5)	-11.8 ▯ (-21.5, -2.06)	77.8 (13.8)	-8.18 • (-17.6, 1.21)	-8.71 (-20.9, 3.45)	-5.09 (-17.2, 6.97)	3.62 (-8.23, 15.5)	0.470

Adj. BL: LME model-adjusted baseline value; Unadj. BL: Unadjusted baseline Mean (SD); MD: Mean difference of changes between groups; p_{int}.: p value based on F test for the interaction between stage and obesity phenotype in the LME model; pairwise contrast p values were adjusted for multiplicity using Tukey's HSD.

† log-transformed; ‡ log1p-transformed in model; For log or log(1 + y)-transformed outcomes, all EMMs and contrasts were back-transformed to the response scale.

• p < .10; ▯ p < .05; ▯ p < .01; ▯ p < .001.

Pulse Analysis Indices: PPI, PDI, OAP

Among the pulse analysis indices except for PTI (Table 5; Fig. 5), only PDI exhibited a significant stage × group interaction ($p_{int} = 0.049$); the interaction terms for PPI and OAP were nonsignificant ($p_{int} = 0.598$ and 0.254, respectively).

PDI increased significantly in the Gynoid group ($+0.73$ mm, $p = 0.004$; $d = 0.75$), with no significant change in the Control or Android groups (both $p > 0.41$). Postexercise, the PDI was significantly greater in the Gynoid group than in the Control group (MD $= +0.94$ mm, $p = 0.004$; $d = 0.84$), indicating a large effect size. PPI and OAP showed no significant interactions or consistent changes (PPI: all $p > 0.22$; OAP: borderline Android vs. Control difference, $p = 0.071$, $d = -0.52$).

Table 5
Response of the PPI, PDI and OAP to submaximal walking by obesity phenotype

		Control		Gynoid		Android		Gynoid - Control	Android - Control	Android - Gynoid	
Features	**Adj. BL**	**Unadj.BL Mean (SD)**	**Change (95% CI)**	**Unadj.BL Mean (SD)**	**Change (95% CI)**	**Unadj.BL Mean (SD)**	**Change (95% CI)**	**MD (95% CI)**	**MD (95% CI)**	**MD (95% CI)**	**p_{int}**
PPI [V]	3.03	3.01 (0.70)	0.15 (-0.14, 0.43)	3.09 (0.70)	0.17 (-0.11, 0.44)	2.99 (0.68)	-0.01 (-0.27, 0.25)	0.02 (-0.32, 0.35)	-0.16 (-0.49, 0.17)	-0.18 (-0.50, 0.15)	0.598
PDI [mm]†	4.67	4.23 (0.94)	-0.21 (-0.76, 0.34)	4.76 (0.84)	0.73 ▯ (0.24, 1.22)	5.21 (1.20)	0.20 (-0.29, 0.68)	0.94 ▯ (0.27, 1.61)	0.41 (-0.26, 1.08)	-0.53 (-1.14, 0.08)	0.049
OAP [V]†	0.69	0.61 (0.12)	0.09 • (-0.01, 0.20)	0.74 (0.15)	-0.01 (-0.10, 0.08)	0.74 (0.10)	-0.02 (-0.11, 0.06)	-0.10 (-0.23, 0.03)	-0.12 • (-0.24, 0.01)	-0.02 (-0.12, 0.08)	0.254

Adj. BL: LME model-adjusted baseline value; Unadj. BL: Unadjusted baseline Mean (SD); MD: Mean difference of changes between groups; p_{int}.: p value based on F test for the interaction between stage and obesity phenotype in the LME model; pairwise contrast p values were adjusted for multiplicity using Tukey's HSD.

† log-transformed; ‡ log1p-transformed in model; For log or log(1 + y)-transformed outcomes, all EMMs and contrasts were back-transformed to the response scale.

• p < .10; ▯ p < .05; ▯ p < .01; ▯ p < .001.

Pulse Analysis Indices: PTI

The six PTIp (where p denotes 20%, 30%, 50%, 70%, 80%, and 90%) displayed a consistent directional pattern after exercise (Table 6; Fig. 6): the Control group tended to increase, the Android group tended to decrease, and the Gynoid group showed little change. Significant stage × group interactions were observed for PTI20 and PTI30 ($p_{int} = 0.032$ and 0.034, respectively); the remaining indices showed nonsignificant interactions (all $p_{int} > 0.15$).

For both interaction-significant indices, those of the Control group increased (PTI20: $d = 0.23$; PTI30: $d = 0.23$), whereas they decreased in the Android group (PTI20: $d = -0.20$; PTI30: $d = -0.21$) after exercise. Postexercise, compared with the Control group, the Android group had significantly lower PTI20 (MD $= -0.37$ mm; $p = 0.001$; $d = -0.86$) and PTI30 (MD $= -0.38$ mm; $p = 0.001$; $d = -0.85$), with large effect sizes. The Gynoid group showed no significant change in either index.

The remaining indices (PTI50 to PTI90) showed a similar directional pattern without significant interactions (all $p_{int} > 0.15$). Postexercise between-group differences favoring Controls over Android were significant at PTI50 ($d = -0.62$), PTI70 ($d = -0.63$), and PTI90 ($d = -0.56$), although these should be interpreted cautiously given the nonsignificant interactions.

Table 6
Responses of PTIp to submaximal walking by obesity phenotype (p = 20%, 30%, 50%, 70%, 80%, and 90%)

		Control		Gynoid		Android		Gynoid - Control	Android - Control	Android - Gynoid	
Features	**Adj. BL**	**Unadj.BL Mean (SD)**	**Change (95% CI)**	**Unadj.BL Mean (SD)**	**Change (95% CI)**	**Unadj.BL Mean (SD)**	**Change (95% CI)**	**MD (95% CI)**	**MD (95% CI)**	**MD (95% CI)**	**p int.**
PTI20 [mm]†	1.48	1.54 (0.40)	0.22 (0.00, 0.43)	1.47 (0.25)	0.05 (-0.15, 0.24)	1.52 (0.32)	-0.15 • (-0.33, 0.02)	-0.17 (-0.43, 0.09)	-0.37 (-0.61, -0.13)	-0.20 • (-0.42, 0.02)	0.032
PTI30 [mm]†	1.25	1.33 (0.42)	0.22 • (-0.00, 0.44)	1.23 (0.27)	0.03 (-0.17, 0.23)	1.31 (0.32)	-0.16 • (-0.34, 0.02)	-0.19 (-0.45, 0.08)	-0.38 (-0.62, -0.13)	-0.19 (-0.41, 0.03)	0.034
PTI50 [mm]†	0.88	0.97 (0.33)	0.13 (-0.05, 0.31)	0.85 (0.27)	0.01 (-0.15, 0.18)	0.96 (0.27)	-0.10 (-0.24, 0.05)	-0.11 (-0.33, 0.10)	-0.22 (-0.42, -0.02)	-0.11 (-0.29, 0.08)	0.166
PTI70 [mm]†	0.55	0.65 (0.29)	0.14 • (-0.00, 0.28)	0.53 (0.21)	0.03 (-0.10, 0.15)	0.66 (0.29)	-0.04 (-0.15, 0.07)	-0.12 (-0.29, 0.06)	-0.18 (-0.35, -0.02)	-0.07 (-0.21, 0.08)	0.150
PTI80 [mm]†	0.42	0.49 (0.23)	0.07 (-0.06, 0.21)	0.42 (0.21)	-0.02 (-0.14, 0.09)	0.51 (0.28)	-0.08 (-0.18, 0.03)	-0.09 (-0.25, 0.06)	-0.15 • (-0.29, 0.00)	-0.05 (-0.18, 0.07)	0.220
PTI90 [mm]‡	0.25	0.27 (0.26)	0.07 (-0.02, 0.17)	0.25 (0.12)	-0.03 (-0.12, 0.06)	0.28 (0.21)	-0.04 (-0.13, 0.05)	-0.10 • (-0.22, 0.01)	-0.11 (-0.22, -0.00)	-0.01 (-0.11, 0.10)	0.176

Adj. BL: LME model-adjusted baseline value; Unadj. BL: Unadjusted baseline Mean (SD); MD: Mean difference of changes between groups; p_{int}.: p value based on F test for the interaction between stage and obesity phenotype in the LME model; pairwise contrast p values were adjusted for multiplicity using Tukey's HSD.

† log-transformed; ‡ log1p-transformed in model; For log or log(1 + y)-transformed outcomes, all EMMs and contrasts were back-transformed to the response scale.

• p < .10; p < .05; p < .01; p < .001.

Discussion

This exploratory study examined radial artery pulse wave responses to a single-stage submaximal treadmill walking test in premenopausal women classified as normal-weight controls, those with gynoid obesity, or those with android obesity. The multidomain analysis revealed three principal observations, each with varying degrees of statistical evidence.

First, the android group showed a within-group pattern suggestive of a blunted postexercise sympathovagal shift: control and gynoid participants exhibited the expected increase in nLF and decrease in nHF, whereas the android group showed no significant changes in frequency-domain HRV. The stage × group interaction for nLF only approached significance (p int = 0.068), and interactions for nHF and LF/HF were also nonsignificant but showed a directionally consistent pattern ($p_{int} = 0.143$ and $p_{int} = 0.153$, respectively); the remaining HRV interactions were clearly nonsignificant ($p_{int} = 0.371$ to 0.826). This pattern should therefore be regarded as a descriptive observation requiring confirmation. The directionality is broadly consistent with prior reports linking central adiposity to altered autonomic reactivity[47,48], although the nonsignificant interactions warrant caution in mechanistic interpretation. We note that LF power contains both sympathetic and vagal contributions and should be interpreted cautiously; therefore, the present data cannot be used to definitively distinguish between reduced sympathetic activation and altered parasympathetic withdrawal in the android group.

In the PTI domain, the evidence for a phenotype-specific exercise response was stronger. PTI is defined as the sensor displacement between the maximum pulse amplitude point and the starting point at which the pulse amplitude first exceeds a prespecified percentage threshold of the maximum, reflecting the overall increasing tendency of pulse pressure as the applied pressure increases and thus serving as a quantitative index of radial pulse tension[49]. PTI20 and PTI30 showed significant stage × group interactions (p int = 0.032 and 0.034,

respectively): these parameters increased in the control group increased but decreased in the android group after exercise, with large between-group effect sizes ($d = -0.86$ and -0.85). These interaction-confirmed results represent the clearest evidence of a differential hemodynamic exercise response associated with android obesity. Importantly, the PTI findings appear to share a common underlying mechanism with the HRV pattern. The postexercise PTI increase in controls likely reflects greater wall pulsatility under augmented cardiac output driven by intact sympathetic activation, whereas the android decrease may indicate that the hemodynamic augmentation was attenuated as a downstream consequence of the blunted autonomic response. Although these two domains did not reach significance simultaneously, the parallel directional pattern and blunted sympathetic activation accompanied by reduced hemodynamic pulsatility suggest that the autonomic and hemodynamic observations may reflect a coherent deficit in cardiovascular reactivity in the context of central adiposity rather than independent findings. The remaining PTI levels (PTI50 to PTI90) showed a similar directional pattern (controls tending upward, android tending downward; see Fig. 7) but without significant interactions (all $p_{int} > 0.15$). Significant postexercise between-group differences were observed at PTI50, PTI70, and PTI90, although these differences should be interpreted with caution given the nonsignificant interactions.

Second, H4 showed the strongest stage × group interaction across all outcomes ($p_{int} = 0.002$), with both obesity groups exhibiting exercise-induced reductions (Gynoid $d = -1.17$; Android $d = -0.79$ vs. Control) that were absent in the controls. Notably, the rAIx@75 pattern differed between the two obesity phenotypes: The Gynoid group participants showed a significant reduction in rAIx@75 (− 11.8%, $p = 0.018$), whereas those in the Android group showed only a borderline trend (− 8.18%, $p = 0.087$), and the stage × group interaction for rAIx@75 was not significant ($p_{int} = 0.470$). This dissociation between H4 and rAIx@75 in the Android group merits attention. Because rAIx@75 is computed as the H3/H1 ratio, its postexercise change depends on the relative magnitudes of changes in both the reflected wave (H3) and the percussive wave (H1). In the Gynoid group, H1 tended to increase after exercise (+ 0.17 V), whereas H3 decreased (− 8.27%), resulting in a clearer reduction in the ratio. In the android group, however, H1 tended to decrease (− 0.19 V), which is consistent with attenuated cardiac output augmentation under blunted sympathetic activation; this attenuated H1 response may have offset the H3 reduction in the ratio, resulting in a nonsignificant change in rAIx@75. H4, being an absolute index rather than a ratio, was less susceptible to this confounding and may have captured the underlying reflection-timing change more directly.

The interpretation that exercise-induced wave reflection changes were shared by both obesity groups is supported by the H4 findings. The augmentation index reflects reflected pressure wave contributions to the systolic waveform, and its postexercise reduction is attributed to decreased reflection magnitude and shifted reflection timing[27,50]. The exercise-induced reductions in H4 and rAIx@75 observed in the obesity groups but not in the controls may reflect altered wave transit properties associated with greater body habitus, such that exercise provocation revealed dynamic differences in wave reflection that were not apparent from resting measurements alone[29,31]. An alternative but complementary interpretation is that normal-weight individuals with intact resting vascular elasticity may have already operated near their dynamic vascular ceiling, leaving limited room for further exercise-induced decreases, whereas the obesity groups retained reserve capacity that became apparent under stimulation. These interpretations are not mutually exclusive.

Third, among the pulse analysis indices, the PDI increased exclusively among participants in the Gynoid group after exercise (+ 0.73 mm, $p = 0.004$; $p_{int} = 0.049$), whereas the Control group showed a nonsignificant decrease (− 0.21 mm), and the Android group showed a nonsignificant increase in the magnitude (+ 0.20 mm), with greater variability. PDI is defined as the sensor displacement from the point of skin contact to the point of maximum pulse amplitude, reflecting the depth at which the radial artery produces its peak pulsatile signal at the measurement site.

The divergent directional pattern across groups is informative. The nonsignificant decrease in the PDI in controls may reflect the relatively superficial position of the radial artery in normal-weight individuals with less surrounding adipose and muscular tissue, such that exercise-induced changes at the measurement site were minimal or resulted in a slight upward shift of the vessel toward the skin surface. In participants in the Android group, the PDI tended to increase in the same direction as that in those in the Gynoid group but to a substantially smaller and nonsignificant degree, which is consistent with attenuated exercise-induced vasodilation under blunted autonomic activation. The significant increase in PDI observed exclusively in participants in the Gynoid group thus appears to represent a phenotype-specific capacity for exercise-induced peripheral vascular adaptation that was neither present in control individuals nor fully expressed in patients with android obesity.

The mechanism underlying the increase in the PDI in the Gynoid group most likely involves exercise-induced radial arterial vasodilation or increased perfusion of the surrounding forearm tissue under augmented cardiac output, both of which are sequelae of intact sympathetic activation. Vasodilation increases vessel diameter and alters the pressure-depth relationship at the measurement site, whereas increased muscular perfusion may alter the mechanical properties of the surrounding tissue, collectively requiring greater sensor displacement to reach the maximum pulse response. This interpretation is supported by the convergent pattern among the participants in the gynoid group, namely, preserved sympathovagal shift, rAIx@75 reduction consistent with peripheral vasodilation, and unique PDI elevation, suggesting that this phenotype retains the capacity for normal exercise-induced peripheral vascular adaptation. The PDI response should therefore be interpreted

as a functional hemodynamic observation consistent with, but not confirming, a broader phenotype-specific difference in exercise-induced vascular adaptation between gynoid and android obesity.

In summary, four interaction-confirmed results, namely, H4 ($p_{int} = 0.002$), PDI ($p_{int} = 0.049$), PTI20 ($p_{int} = 0.032$), and PTI30 ($p_{int} = 0.034$), provide the strongest evidence that exercise-induced pulse wave changes differ by obesity phenotype. The remaining observations (descriptive autonomic divergence in the Android group, H4–rAIx@75 dissociation in the Android group, higher-threshold PTI trends) are patterns consistent with, but not formally confirming, a broader phenotype-specific response[18,19]; these should be treated as hypotheses for future testing rather than established findings.

Across these domains, a coherent phenotype-dependent picture emerges. Android obesity is characterized by blunted autonomic reactivity coupled with reduced hemodynamic pulsatility (PTI) and attenuated cardiac output augmentation (H1 direction), suggesting a centrally mediated deficit in cardiovascular reactivity consistent with the known autonomic and vascular consequences of visceral adiposity[18,19,47]. In contrast, gynoid obesity preserved the central autonomic exercise response and resulted in intact hemodynamic augmentation, while peripheral morphological changes unique to this phenotype, namely, a significant increase in the PDI and a significant decrease in rAIx@75, were observed, and both these changes are consistent with those associated with exercise-induced peripheral vasodilation. The H4 reduction shared by participants in both obesity groups but absent in control individuals, may represent a common effect of excess body mass on wave transit properties that is independent of fat distribution. Taken together, these findings suggest that body fat distribution, rather than excess adiposity alone, shapes the integrated autonomic-vascular response to acute exercise.

This study had several limitations. The small sample (N = 42; 13–15 per group) limited statistical power, and the exploratory cross-sectional design made the findings hypothesis-generating rather than confirmatory; preexisting vascular remodeling cannot be disentangled from acute functional responses. The obesity phenotype was classified by WHR with an intentional exclusion gap (0.85–0.90), which sharpened the phenotypic contrast but limits generalizability; visceral and subcutaneous adipose volumes were not directly imaged. Although Visit 2 was scheduled during the follicular phase (within 10 days after the onset of menstruation) to reduce hormonal variability, the actual cycle phase was not biochemically verified, and residual hormonal fluctuations may have modulated autonomic tone, arterial stiffness, and peripheral vascular reactivity[51–54]. Pulse waves were obtained at a single postexercise time point (~ 3 minutes after cessation), capturing only the early recovery phase. Furthermore, 25 outcomes were analyzed across three domains without formal correction for multiple comparisons across the full variable set; these findings require confirmation in independent samples. Finally, radial artery measurements may not be directly extrapolated to central aortic hemodynamics.

Conclusion

In this exploratory study, premenopausal women with android and gynoid obesity exhibited distinct radial artery pulse wave response patterns following submaximal treadmill walking, with four outcomes showing significant stage × group interactions. Participants in both obesity groups showed exercise-induced reductions in incisura height (H4) that were absent in normal-weight controls, which is consistent with a common effect of excess body mass on wave transit properties that is independent of fat distribution pattern. Android obesity was characterized by a coherent pattern of blunted autonomic reactivity and reduced hemodynamic pulsatility: participants in the Android group failed to exhibit the postexercise sympathovagal shift seen in those in the Control and Gynoid groups and showed divergent decreases in pulse tension indices at lower pressure thresholds (PTI20, PTI30), suggesting a centrally mediated deficit in cardiovascular reactivity associated with central adiposity. The dissociation between H4 and rAIx@75 in the android group, where H4 decreased significantly but rAIx@75 did not, further highlights that attenuated cardiac output augmentation under blunted autonomic activation may obscure ratio-based indices while leaving absolute waveform markers intact. In contrast, gynoid obesity preserved the autonomic exercise response and was uniquely associated with increased pulse depth (PDI) after exercise, which is consistent with exercise-induced peripheral vasodilation and increased forearm tissue perfusion as sequelae of intact sympathetic activation. Collectively, these findings suggest that body fat distribution, rather than excess adiposity alone, shapes the integrated autonomic-vascular response to acute exercise in premenopausal women and that physiological provocation with multiparameter pulse wave analysis may reveal vascular phenotype differences that are not apparent from resting measurements. Verification in larger, prospectively designed studies with direct adipose tissue quantification and multiple postexercise time points is warranted.

Declarations

Conflict of Interest Statement

The authors declare that they have no conflicts of interest.

Ethics and Clinical Trial Registration

This study was approved by the institutional review board at Wonkwang University Gwangju Medical Center (approval number: WKIRB-2015/8). The study was registered with the Clinical Research Information Service (CRIS), Republic of Korea (registration number: KCT0001676).

Funding

This work was supported by the Korea Institute of Oriental Medicine (KIOM) under Grant KSN2512012 funded by the Ministry of Science and ICT, Republic of Korea, and by the National Research Council of Science and Technology (NST) through the Aging Convergence Research Center (Grant No. CRC22015-500).

Author Contribution

BK and YJJ conceived and designed the study. BK conducted the study, collected the data, performed the data analysis, and drafted the manuscript. JHB provided expertise on pulse wave analysis and contributed to data interpretation. SL supervised the experiments and contributed to manuscript revision. YJJ secured funding, oversaw project administration, supervised the research team, and contributed to manuscript writing and editing. All the authors contributed to the article and approved the submitted version.

Data Availability

The datasets generated and/or analysed during the current study are available from the corresponding author on reasonable request.

References

1. Tsao, C. W. et al. Heart disease and stroke statistics—2023 update: A report from the american heart association. *Circulation* **147**, e93–e621 (2023).
2. Roth, G. A. et al. Global burden of cardiovascular diseases and risk factors, 1990–2019. *J. Am. Coll. Cardiol.* **76**, 2982–3021 (2020).
3. Vague, J. The degree of masculine differentiation of obesities: A factor determining predisposition to diabetes, atherosclerosis, gout, and uric calculous disease. *Am. J. Clin. Nutr.* **4**, 20–34 (1956).
4. Björntorp, P. Regional patterns of fat distribution. *Ann. Intern. Med.* **103**, 994–995 (1985).
5. Jensen, M. D. Role of body fat distribution and the metabolic complications of obesity. *J. Clin. Endocrinol. Metabolism*. **93**, s57–s63 (2008).
6. Kissebah, A. H. et al. Relation of body fat distribution to metabolic complications of obesity. *J. Clin. Endocrinol. Metabolism*. **54**, 254–260 (1982).
7. Larsson, B. et al. Abdominal adipose tissue distribution, obesity, and risk of cardiovascular disease and death: 13-year follow-up of participants in the study of men born in 1913. *Br. Med. J. (Clin Res. Ed)*. **288**, 1401–1404 (1984).
8. Lapidus, L. et al. Distribution of adipose tissue and risk of cardiovascular disease and death: A 12-year follow-up of participants in the population study of women in gothenburg, sweden. *Br. Med. J. (Clin Res. Ed)*. **289**, 1257–1261 (1984).
9. Sari, C. I. et al. Android fat deposition and its association with cardiovascular risk factors in overweight young males. *Frontiers Physiology* **10**, (2019).
10. Klarqvist, M. D. R. et al. Silhouette images enable estimation of body fat distribution and associated cardiometabolic risk. *npj Digit. Med.* **5**, 1–9 (2022).
11. World Health Organization. *Obesity: Preventing and Managing the Global Epidemic: Report of a WHO Consultation* (World Health Organization, 2000).
12. de Koning, L., Merchant, A. T., Pogue, J. & Anand, S. S. Waist circumference and waist-to-hip ratio as predictors of cardiovascular events: Meta-regression analysis of prospective studies. *Eur. Heart J.* **28**, 850–856 (2007).
13. Czernichow, S., Kengne, A. P., Stamatakis, E., Hamer, M. & Batty, G. D. Body mass index, waist circumference and waist–hip ratio: Which is the better discriminator of cardiovascular disease mortality risk? Evidence from an individual-participant meta-analysis of 82 864 participants from nine cohort studies. *Obes. Rev.* **12**, 680–687 (2011).

14. Romero-Corral, A. et al. Modest visceral fat gain causes endothelial dysfunction in healthy humans. *J. Am. Coll. Cardiol.* **56**, 662–666 (2010).
15. Kim, H. L. et al. Association between body fat parameters and arterial stiffness. *Sci. Rep.* **11**, 20536 (2021).
16. Chao, H. et al. Impact of obesity phenotype on central aortic hemodynamics and arterial stiffness in a chinese health assessment population. *RCM* **23**, 216 (2022).
17. Antonio-Villa, N. E. et al. Visceral adipose tissue is an independent predictor and mediator of the progression of coronary calcification: A prospective sub-analysis of the GEA study. *Cardiovasc. Diabetol.* **22**, 81 (2023).
18. Koenen, M., Hill, M. A., Cohen, P. & Sowers, J. R. Obesity, adipose tissue and vascular dysfunction. *Circul. Res.* **128**, 951–968 (2021).
19. Suh, H. S. et al. Vascular endothelial dysfunction tested by blunted response to endothelium-dependent vasodilation by salbutamol and its related factors in uncomplicated pre-menopausal obese women. *Int. J. Obes.* **29**, 217–222 (2005).
20. Yang, J. et al. Analysis of the radial pulse wave and its clinical applications: A survey. *IEEE Access.* **9**, 157940–157959 (2021).
21. King, E., Cobbin, D., Walsh, S. & Ryan, D. The reliable measurement of radial pulse characteristics. *Acupunct. Med.* **20**, 150–159 (2002).
22. Bilton, K. & Zaslawski, C. Reliability of manual pulse diagnosis methods in traditional east asian medicine: A systematic narrative literature review. *J. Altern. Complement. Med.* **22**, 599–609 (2016).
23. Obeid, H. et al. Radial-digital pulse wave velocity: A noninvasive method for assessing stiffness of small conduit arteries. *Am. J. Physiol. Heart Circ. Physiol.* **320**, H1361–H1369 (2021).
24. Meng, K. et al. Wearable pressure sensors for pulse wave monitoring. *Adv. Mater.* **34**, 2109357 (2022).
25. Zhang, C. et al. Identifying coronary artery lesions by feature analysis of radial pulse wave: A case-control study. *BioMed Research International* e5047501 (2021). (2021).
26. Javorka, M., Zila, I., Balhárek, T. & Javorka, K. Heart rate recovery after exercise: Relations to heart rate variability and complexity. *Braz J. Med. Biol. Res.* **35**, 991–1000 (2002).
27. Gkaliagkousi, E., Gavriilaki, E., Nikolaidou, B., Triantafyllou, G. & Douma, S. Exercise-induced pulse wave velocity changes in untreated patients with essential hypertension: The effect of an angiotensin receptor antagonist. *J. Clin. Hypertens.* **16**, 482–487 (2014).
28. Barros, J. P. et al. The effects of acute aerobic exercise on blood pressure, arterial function, and heart rate variability in men living with HIV. *Front. Physiol.* **12**, 685306 (2021).
29. Sun, H., Zhang, Y. & Shi, L. Advances in exercise-induced vascular adaptation: Mechanisms, models, and methods. *Front. Bioeng. Biotechnol.* **12**, 1370234 (2024).
30. Huang, Z. et al. The effect of acute aerobic exercise on arterial stiffness in individuals with different body fat percentages: A cross-sectional study. *Front. Cardiovasc. Med.* **9**, 1072191 (2023).
31. Bunsawat, K. et al. The effect of acute maximal exercise on postexercise hemodynamics and central arterial stiffness in obese and normal-weight individuals. *Physiological Rep.* **5**, e13226 (2017).
32. WHO Expert Consultation. Appropriate body-mass index for asian populations and its implications for policy and intervention strategies. *Lancet* **363**, 157–163 (2004).
33. Kim, M. K. et al. Defining obesity and overweight using BMI in the Korean population: A review. *J. Korean Med. Sci.* **29**, 1514–1521 (2014).
34. Manigrasso, M. R. et al. Association between circulating adiponectin and interleukin-10 levels in android obesity: Effects of weight loss. *J. Clin. Endocrinol. Metabolism*. **90**, 5876–5879 (2005).
35. Pinkhasov, B. B., Selyatitskaya, V. G., Karapetyan, A. R. & Astrakhantseva, E. L. Metabolic syndrome in men and women with upper or lower types of body fat distribution. *Health* **4**, 1381–1389 (2012).
36. Korean Agency for Technology and Standards. Size korea: Korean human body dimension survey. (2015).
37. Ebbeling, C. B., Ward, A., Puleo, E. M., Widrick, J. & Rippe, J. M. Development of a single-stage submaximal treadmill walking test. *Med. Sci. Sports Exerc.* **23**, 966–973 (1991).
38. Nes, B. M., Janszky, I., Wisløff, U., Støylen, A. & Karlsen, T. Age-predicted maximal heart rate in healthy subjects: The HUNT fitness study. *Scand. J. Med. Sci. Sports*. **23**, 697–704 (2013).
39. Kim, T. H. et al. Hemodynamic changes caused by acupuncture in healthy volunteers: A prospective, single-arm exploratory clinical study. *BMC Complement. Altern. Med.* **17**, 274 (2017).
40. Bae, J. H. et al. Radial pulse and electrocardiography modulation by mild thermal stresses applied to feet: An exploratory study with randomized, crossover design. *Chin. J. Integr. Med.* **26**, 299–306 (2020).
41. Bae, J. H. & Jeon, Y. J. Pulse sharpness as a quantitative index of vascular aging. *Sci. Rep.* **11**, 19895 (2021).
42. R Core Team. *R: A Language and Environment for Statistical Computing* (R Foundation for Statistical Computing, 2026).

43. Senn, S. Change from baseline and analysis of covariance revisited. *Stat. Med.* **25**, 4334–4344 (2006).
44. Van Breukelen, G. J. P. ANCOVA versus change from baseline: More power in randomized studies, more bias in nonrandomized studies. *J. Clin. Epidemiol.* **59**, 920–925 (2006).
45. Lenth, R. V. & Piaskowski, J. *Emmeans: Estimated Marginal Means, Aka Least-Squares Means*. (2026). 10.32614/CRAN.package.emmeans
46. Rosenthal, R. Parametric measures of effect size. in The handbook of research synthesis (eds (eds Cooper, H. & Hedges, L. V.) 231–244 (Russell Sage Foundation, New York, (1994).
47. Grassi, G., Mark, A. & Esler, M. Relevance of sympathetic nervous system activation in obesity and metabolic syndrome. *Curr. Hypertens. Rep.* **17**, 36 (2015).
48. Farah, B. Q., Prado, W. L., do, Tenório, T. R., dos, S. & Ritti-Dias, R. M. Heart rate variability and its relationship with central and general obesity in obese normotensive adolescents. *Einstein (São Paulo)*. **11**, 285–290 (2013).
49. Kim, J. et al. A comparative study of the radial pulse between primary dysmenorrhea patients and healthy subjects during the menstrual phase. *Sci. Rep.* **9**, 9716 (2019).
50. Rasool, G. H., Kimoto, A., Phan, C., Morita, M. & Sugawara, J. Lower-body dynamic exercise reduces wave reflection in healthy young adults. *Appl. Physiol. Nutr. Metab.* **46**, 1405–1411 (2021).
51. Ramesh, S. et al. Heart rate variability as a function of menopausal status, menstrual cycle phase, and estradiol level. *Physiological Rep.* **10**, e15298 (2022).
52. de Zambotti, M., Trinder, J., Colrain, I. M. & Baker, F. C. Menstrual cycle-related variation in autonomic nervous system functioning in women in the early menopausal transition with and without insomnia disorder. *Psychoneuroendocrinology* **75**, 44–51 (2016).
53. Williford, K. T., Frye, E. V. & Kappus, R. M. The effects of previous amenorrhea on endothelial and vascular function. *International Journal of Endocrinology* 6305659 (2025). (2025).
54. Mascone, S. E., Chesney, C. A., Eagan, L. E. & Ranadive, S. M. Similar inflammatory response and conduit artery vascular function between sexes following induced inflammation. *Exp. Physiol.* **106**, 2276–2285 (2021).

Figures

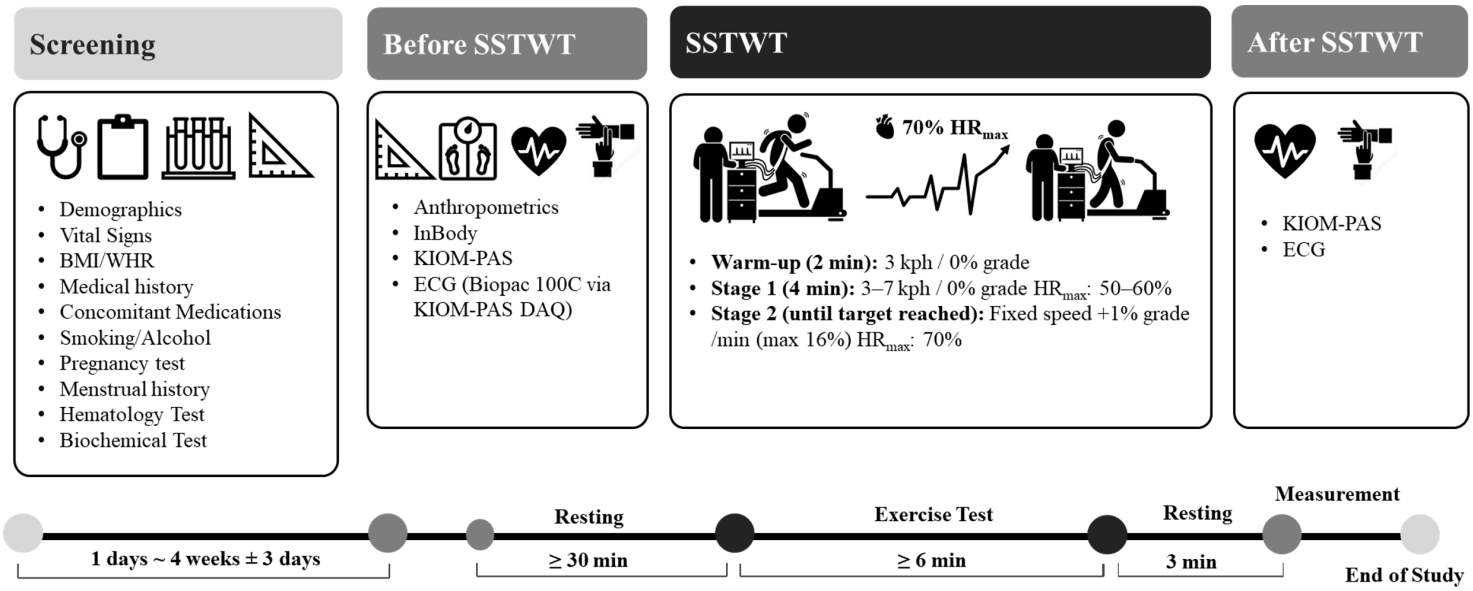


Figure 1

Scheme of the single-stage submaximal treadmill walking test protocol, including warm-up, workload progression, and the target of 70% age-predicted maximal heart rate.

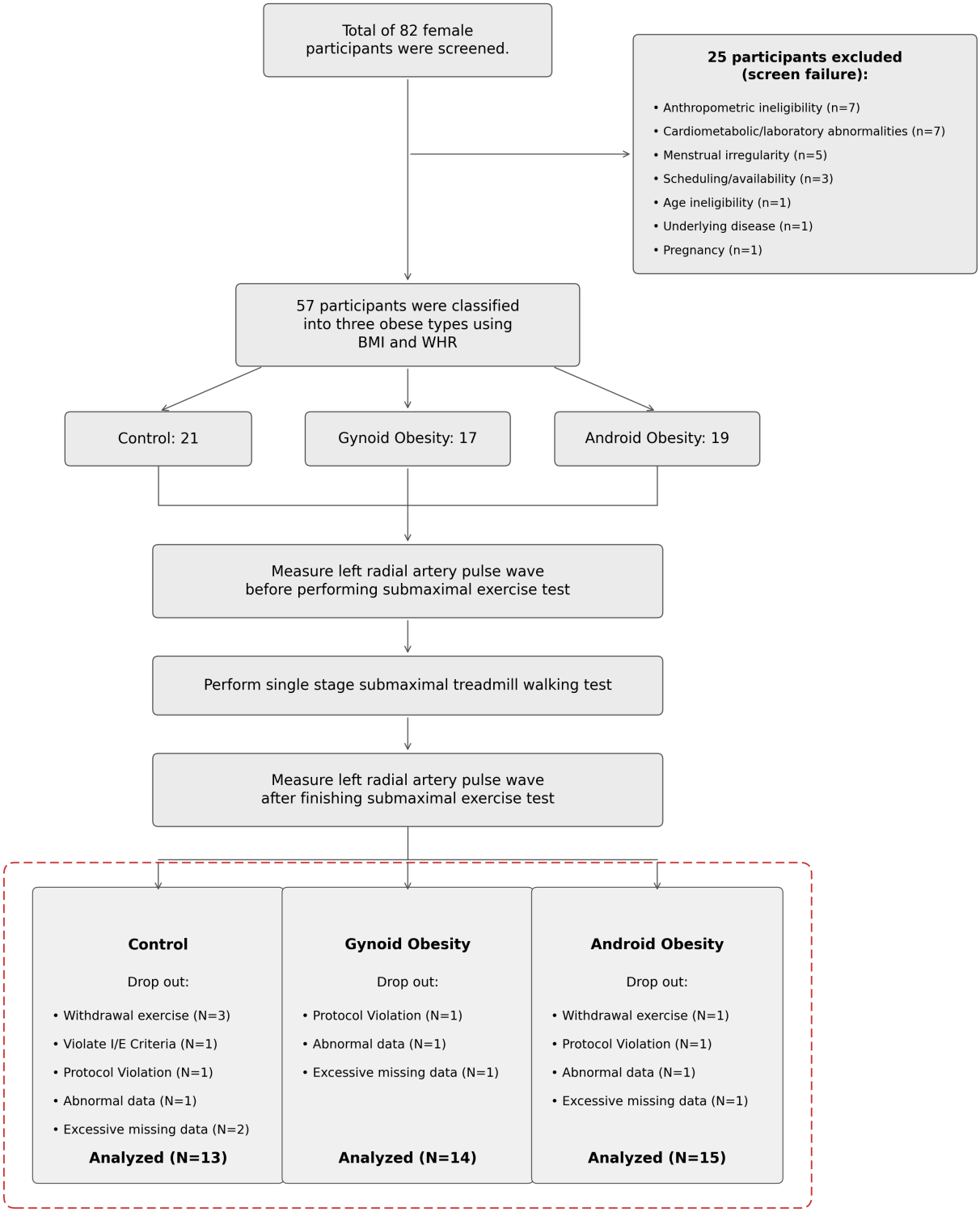


Figure 2

Flow diagram of participant screening, enrollment, and analysis set derivation.

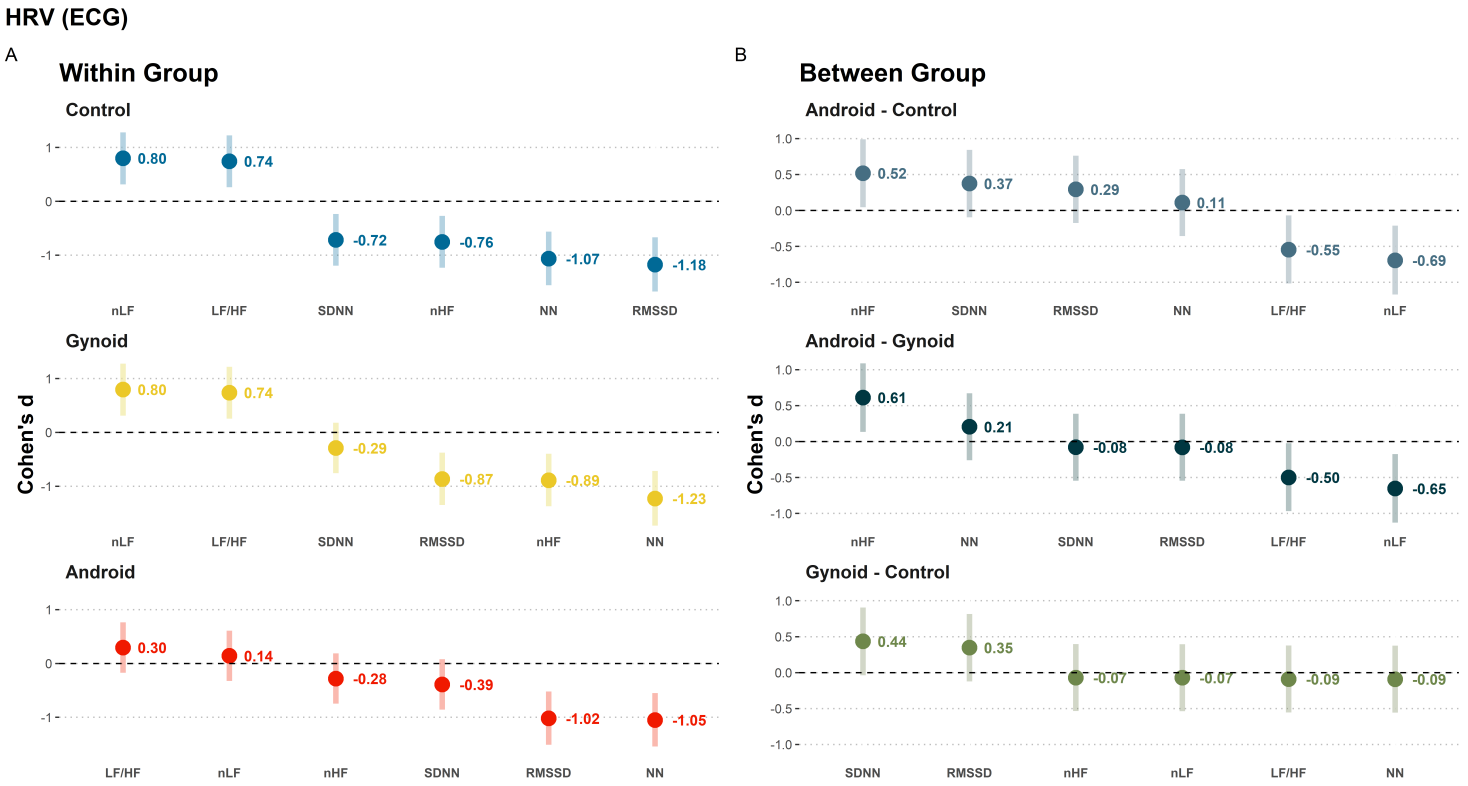


Figure 3

Cohen's d effect sizes for HRV metrics (A) Within-group changes from baseline to postexercise. (B) Between-group differences in exercise-induced changes.

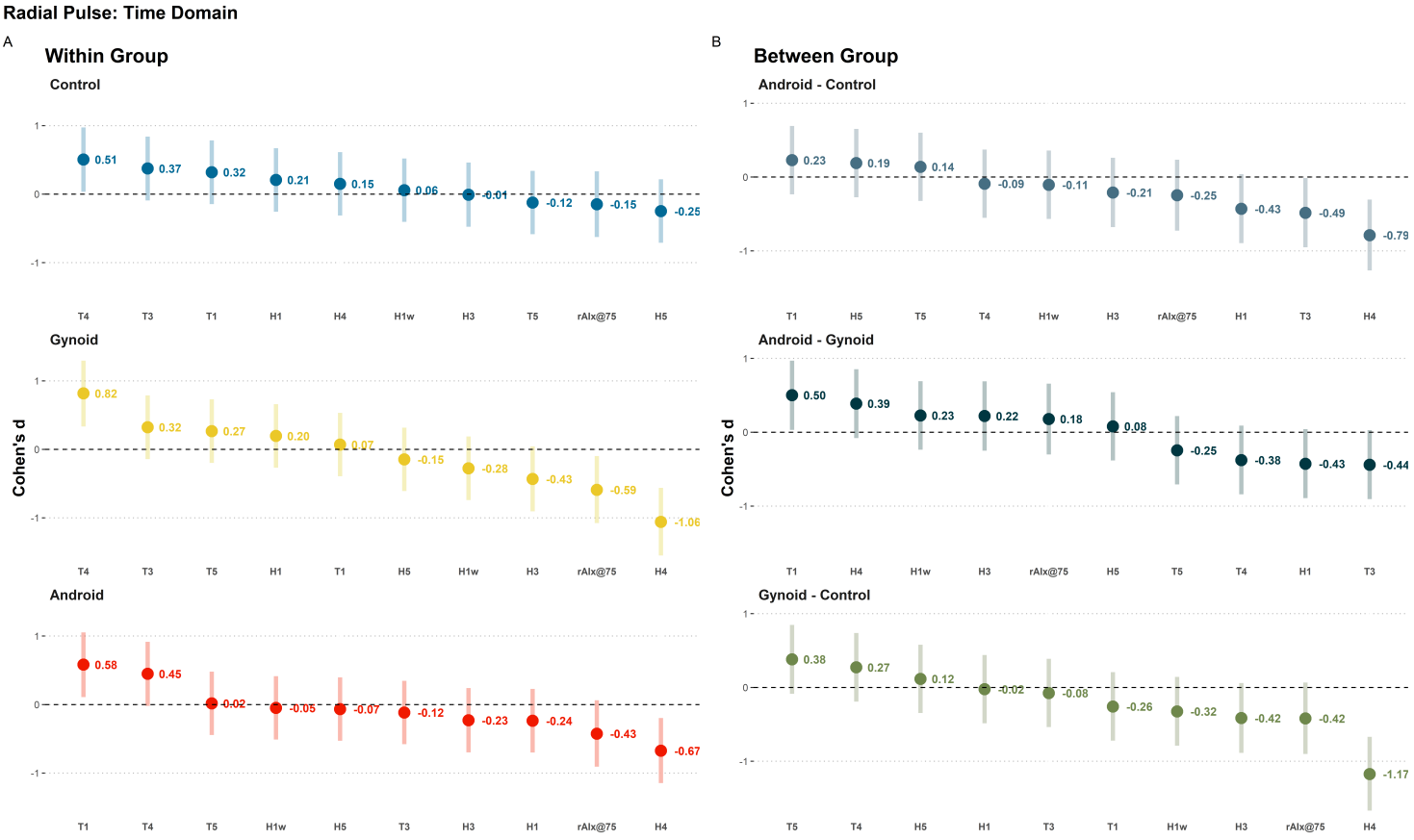


Figure 4

Cohen's d effect sizes for time-domain pulse waveform features. (A) Within-group changes from baseline to postexercise. (B) Between-group differences in exercise-induced changes.

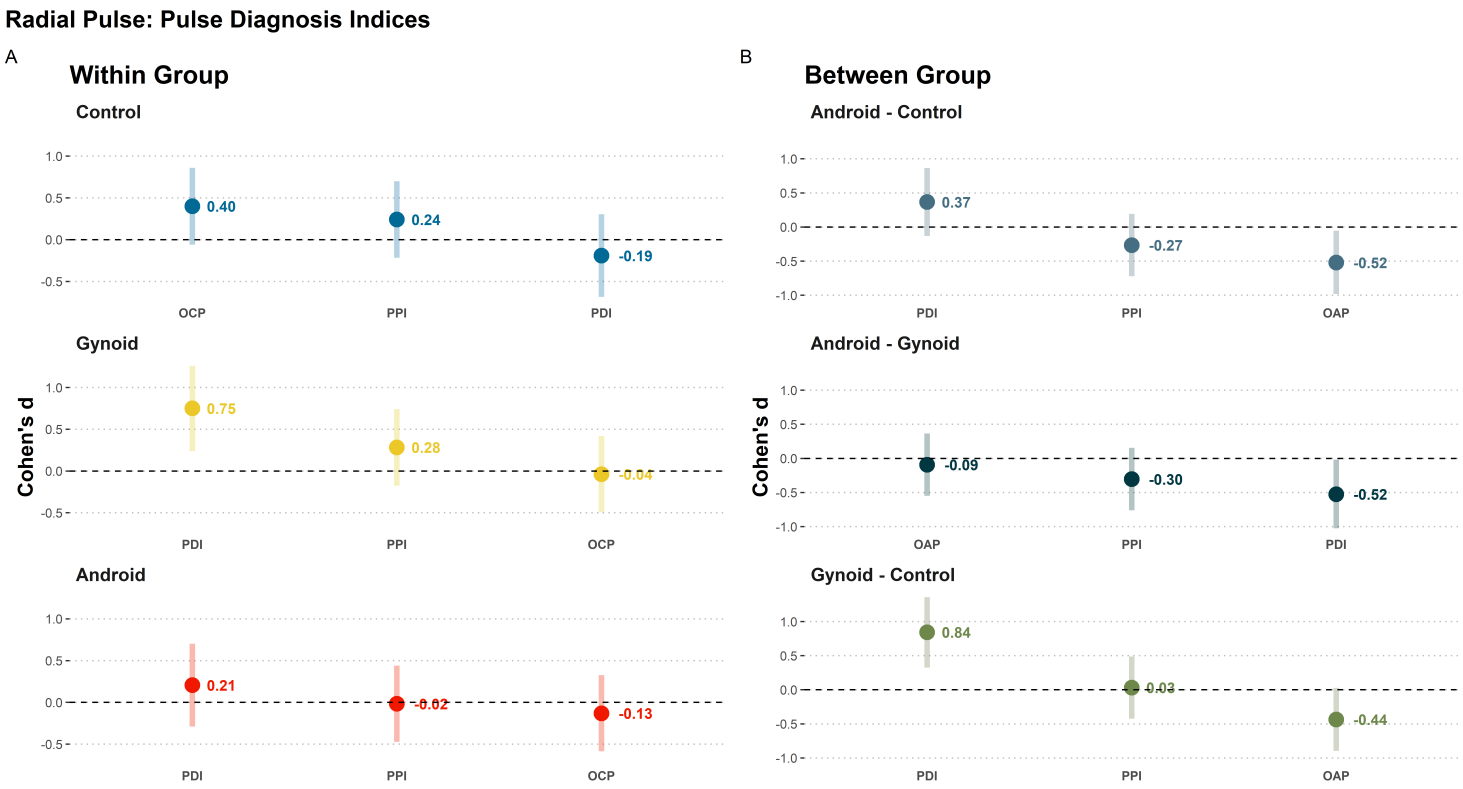


Figure 5

Cohen's d effect sizes for pulse analysis indices (PPI, PDI, OAP). (A) Within-group changes from baseline to postexercise. (B) Between-group differences in exercise-induced changes.

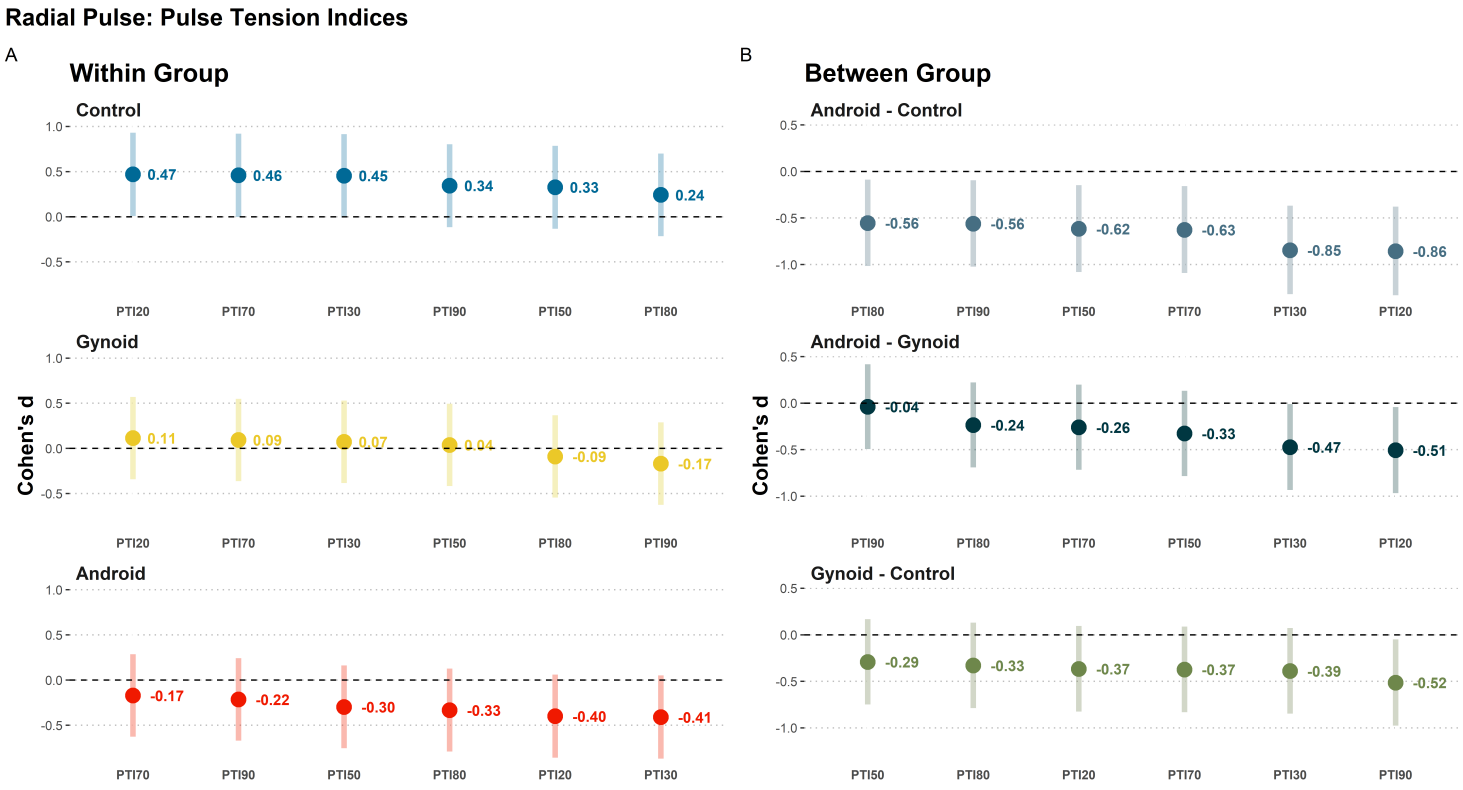


Figure 6

Cohen's d effect sizes for pulse tension indices. (A) Within-group changes from baseline to postexercise. (B) Between-group differences in exercise-induced changes.

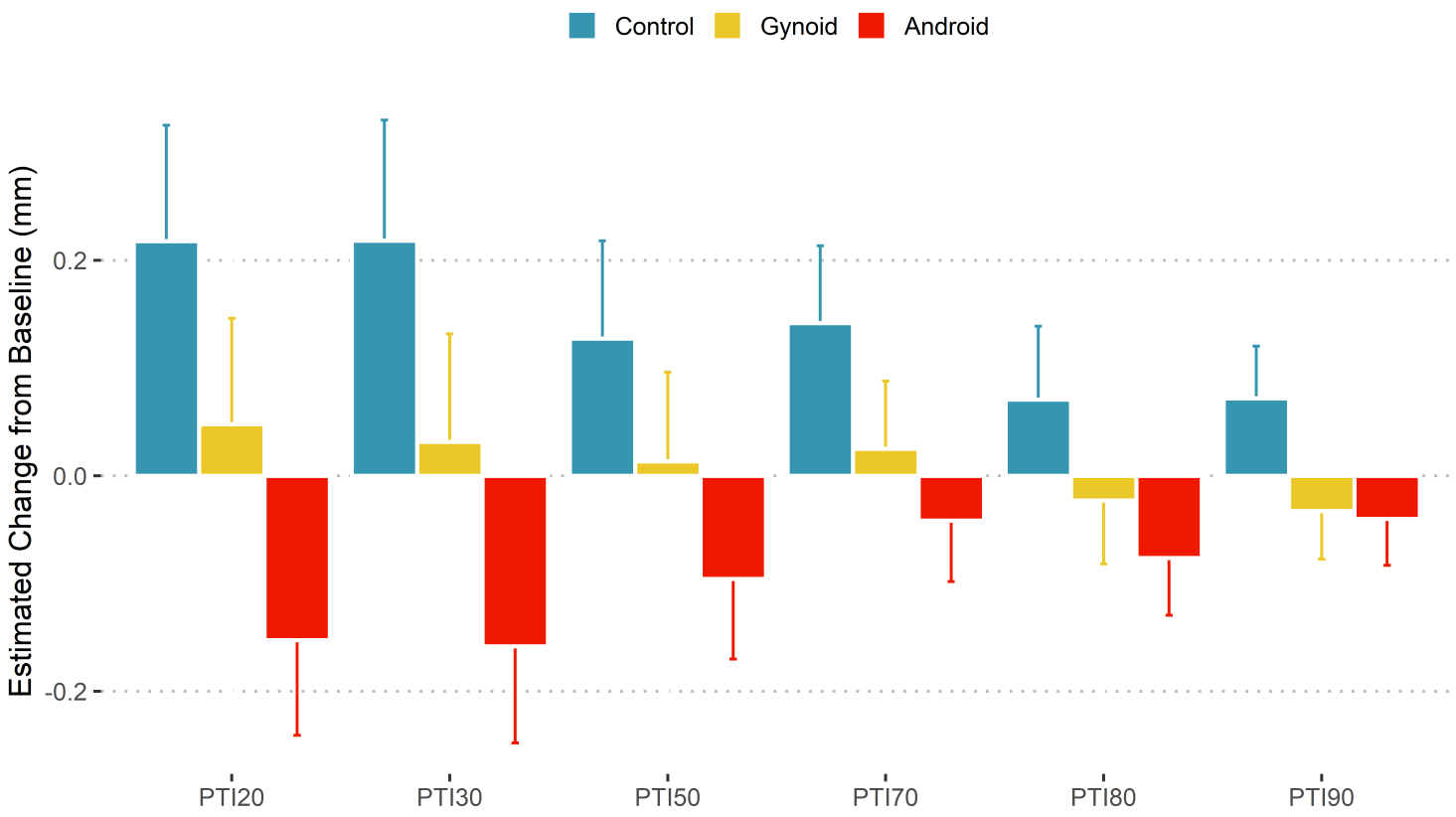


Figure 7

Estimated changes from baseline to postexercise for pulse tension indices by obesity phenotype. Error bars represent standard errors of the estimates.